Article

Not peer-reviewed version

Estimation of Seasonal Freshwater Inflows in Coastal Southern India using Stable Isotope Analysis and Machine Learning Techniques

Prasanna K. , Ravi Rangarajan * , Fursan Thabit , Prosenjit Ghosh , Habeeb Rahman

Posted Date: 19 May 2025

doi: 10.20944/preprints202505.1362.v1

Keywords: Seasonal Freshwater Flux; Stable Isotopes; Machine Learning; Salinity; Estuarine Dynamics

 doi:10.20944/preprints202505.1362.v1

Article

Estimation of Seasonal Freshwater Inflows in Coastal Southern India using Stable Isotope Analysis and Machine Learning Techniques

Prasanna K. [1], Ravi Rangarajan [2,3,*], Fursan Thabit [3,4], Prosenjit Ghosh [5,6,7] and Habeeb Rahman [8]

[1] Birbal Sahni Institute of Palaeosciences, Lucknow – 226007, India
[2] Department of Environmental Health and Safety, University of Doha for Science and Technology, Doha, Qatar
[3] Centre for Excellence in Sustainability and Food Security, University of Doha for Science and Technology, Doha, Qatar
[4] National Computer Network Intrusion Protection Center University of Chinese Academy of Sciences, Beijing, China
[5] Centre for Earth Sciences, Indian Institute of Science, Bangalore – 560 012, India
[6] Divecha Centre for Climate Change, Indian Institute of Science, Bangalore - 560 012, India
[7] Interdisciplinary Centre for Water Research, Indian Institute of Science, Bangalore - 560012, India
[8] Department of Chemical Oceanography, Cochin University of Science and Technology, Cochin - 682022, India
* Correspondence: ravi.rangarajan@udst.edu.qa

Abstract: Cochin backwater region in Southern India is one of the most dynamic estuaries, strongly influenced by seasonal river runoff and seawater intrusion. This study explores the relationship between monsoonal rains, salinity, and stable isotopic composition ($\delta^{18}O$ and $\delta^{13}C$) to estimate the contribution of freshwater fluxes at different seasonal intervals for the Cochin Backwater (CBW) estuary. Seasonal variations in oxygen isotopes and salinity revealed distinct trends indicative of freshwater-seawater mixing dynamics. The comparison of Local and Global Meteoric Water Lines highlighted enriched isotope values during the pre-monsoon season, showing significant evaporation effects. Carbon (C) isotopic analysis in dissolved inorganic matter ($\delta^{13}C_{DIC}$) at 17 stations during the pre-monsoon season revealed spatially distinct carbon dynamics zones, influenced by various sources. These characteristic zones were; Zone 1, dominated by seawater, exhibited heavier $\delta^{13}C_{DIC}$ values; Zone 2 showing significant contributions of lighter terrestrial $\delta^{13}C$; while Zone 3 reflected inputs from regional and local paddy fields with a distinct C_3 isotopic signature (-25‰), modified by estuarine productivity. In addition, different advanced machine learning techniques were tested to improve analysis and prediction of seasonal variations in isotopic composition and salinity. The combination of these advanced machine learning models not only improved the predictive accuracy of seasonal freshwater fluxes but also provided a robust framework for understanding the estuarine ecosystem, and would pave way for better management and conservation strategies.

Keywords: seasonal freshwater flux; stable isotopes; machine learning; salinity; estuarine dynamics

1. Introduction

Estuaries are dynamic systems adjacent to coastal regions that exhibit seasonal variability in productivity due to differential fluxes of freshwater from rivers. Globally, estuaries function as crucial interfaces between terrestrial and marine ecosystems, supporting high biodiversity and providing ecosystem services such as nutrient cycling, carbon sequestration, and fisheries support [1]. Monsoonal estuaries, a semi-enclosed coastal body of water that has a free or regulated

 doi:10.20944/preprints202505.1362.v1

connection with the open sea, is a unique feature in southern India. These monsoonal estuaries offer an environment for understanding freshwater fluxes due to the characteristic mixing pattern denoting differential seawater influx, and freshwater input from continental runoff. The seasonal hydrological variability observed in monsoonal estuaries of southern India mirrors patterns in other estuarine systems worldwide, such as the Mekong Delta in Southeast Asia and the Amazon Estuary in South America, where freshwater influx, tidal regimes, and anthropogenic pressures collectively shape estuarine dynamics [1,2]. Comparative studies across these diverse geographic regions can enhance our understanding of estuarine resilience and responses to climate change and human activities on a global scale [3]. In that context, the current study was conducted in one of the largest monsoonal estuaries in southern Indian i.e., Cochin Back Water (CBW) estuary [4,5]. Tides in these estuaries are semi-diurnal with an average tidal height of 1 m, and the impact of anthropogenic interventions on the estuarine system is rather high and its geochemical dynamics is well-studied [5–8].

Freshwater entry into the CBW estuary occurs primarily through six rivers, Periyar, Muvattupuzha, Pampa, Achankovil, Manimala, and Meenachil. During the dry season, the runoff from the upstream area is minimal, promoting saline water intrusion into the low-lying paddy fields of CBW [9]. Unlike perennial rivers, such as Hooghly, which drain into the Bay of Bengal, forming an estuary near Sunderban [10], Southern Indian rivers are devoid of any glacial meltwater input during dry seasons. The contribution of freshwater to the estuary can be estimated at seasonal time intervals by differential mixing of seawater and freshwater, and this process can be quantified using data on salinity and $\delta^{18}O$ ratio in estuary water [11,12]. Stable isotopic approaches, particularly the use of $\delta^{18}O$, δD, and $\delta^{13}C$ signatures, have proven to be robust tools in tracing water sources, salinity gradients, and biogeochemical dynamics across diverse estuarine systems worldwide, providing critical insights into the effects of climate variability, land use change, and anthropogenic pressure on estuarine carbon cycling [13,14]. While $\delta^{18}O$ and δD ratios are useful in predicting the mixing and evaporation processes, $\delta^{13}C$ in Dissolved Inorganic Carbon (DIC) enable an understanding of both mixing and productivity or carbon uptake by the biota in the estuarine system [10].

Analysis of stable isotope data coupled with advanced machine learning techniques will enhance the analysis and prediction of seasonal variations in isotopic composition and salinity [15,16]. AI techniques, such as Artificial Neural Networks (ANN), Adaptive Neuro-Fuzzy Inference Systems (ANFIS), Support Vector Machines (SVM), Radial Function Based Neural Network (RBNN), Random Forest (RF), K-Nearest Neighbour (KNN) have become increasingly popular for addressing complex problems across various research domains [15–19]. These techniques excel at modeling complex nonlinear systems, effectively compensating for the limitations of traditional numerical models. ANN, ANFIS, and SVM are advanced computational techniques increasingly applied in the study of stable isotopes in estuarine environments. These methods enhance the understanding of complex ecological interactions and isotopic compositions, providing valuable insights into environmental changes. ANNs are effective in modelling complex ecosystems, as demonstrated in studies predicting phytoplankton blooms in estuaries [18]. SVMs have been utilized alongside ANNs to estimate isotopic compositions, salinity, and temperature, showing competitive accuracy in predictions [15].

In a particular case study from the Mediterranean Sea, three predictive models were developed using ANN, RF and SVM involving five key variables: (i–ii) geographic coordinates (longitude and latitude), (iii) year, (iv) month, and (v) depth. Among these, RF model demonstrated the highest prediction accuracy during the querying phase, achieving a mean absolute percentage error (MAPE) of approximately 4.98% for isotope composition, below 0.20% for salinity, and around 2.44% for temperature. Despite the advantages of these computational techniques and their predication accuracy, traditional methods still play a crucial role in hydro-environmental research, particularly in validating and complementing findings from machine learning models [15]. Employing AI models for δD and $\delta^{18}O$ estimation of freshwater seawater interplay in the estuarine system in the Asian context is very much lacking, and the current study would represent a novel and valuable

 doi:10.20944/preprints202505.1362.v1

contribution to the costal research literature in the Asian region. The objective of using machine learning algorithms in this study was to develop a simple, and accurate model for estimating $\delta^{18}O$ and $\delta^{13}C$ isotopes in the CBW estuary. This was achieved by employing advanced machine learning techniques, including Gradient Boosting Machines (GBM), Gaussian Process Regression (GPR), Classification and Regression Tree (CART), and Extreme Learning Machines (ELM) [20–22]. These models were chosen for their ability to capture non-linear relationships, handle high-dimensional data, and quantify uncertainties in predictions. The models were rigorously evaluated for their accuracy, efficiency, and potential to serve as reliable alternatives to traditional isotope analysis methods, offering a robust framework for understanding seasonal freshwater fluxes and estuarine dynamics of the India sub-continent.

In the current study, we explored the relationship between salinity, stable isotopic composition, and freshwater fluxes in the CBW estuary across different seasons. We used existing data from the Arabian Sea to establish seawater $\delta^{18}O$ and salinity baselines [23,24] and adopted seasonal rainwater composition from previous studies [25]. By analyzing productivity patterns and their link to salinity and freshwater input ($\delta^{18}O$), we identified distinct zones within the estuary based on varying freshwater influence and productivity levels. To classify these estuarine zones, we combined salinity and isotope data with spatial and temporal patterns, and used applied machine learning techniques like GBM, GPR, CART and ELM, and conventional machine learning techniques like RF, KNN, SVM to model and predict changes in isotopic composition, and evaluate the performance metrics of the used techniques

2. Materials and Methods

2.1. Study Area

Based on its dimensions, CBW is the largest estuarine system along the west coast of India and belongs to the Vembanad-Kol wetland system, one of the three Ramsar sites in Kerala that extends from Munambam (10° 10' 00" N, 76°10' 15" E) in the north to Alappuzha (09° 30' 00" N, 76° 28' 10" E) in the south for 96.5 km in length (Figure 1). The width varies from 450 m to 4 km, and the depth ranges from 15 m at the Cochin Inlet to 3 m near the head, with an average depth of 1.5 meters. The barrier spits are interrupted by tidal inlets at two locations (i) Munambam inlet in the north and (ii) Cochin inlet in the middle.

The present study was conducted on CBW and Vembanad Lake, situated at the southern tip of the Indian subcontinent. This region experiences three distinct seasons: Pre-Monsoon (PM, April–May), Southwest Monsoon (SWM, June–September), and Northeast Monsoon (NEM, October–December). During the monsoon season, the influx of freshwater significantly increases due to heavy precipitation, while the non-monsoon season (January–March) is characterized by reduced riverine input and dominant tidal forcing, leading to higher salinity levels in the estuary [11,26]. Water samples for $\delta^{18}O$ and salinity analysis were collected fortnightly during high and low tides for a 1-year period between October to September of subsequent year (Table 1). Additionally, a spatial survey covering 17 sites (Figure 1, Table 2) was conducted in the pre-monsoon period (March-May) to document variability in isotopic composition and salinity.

 doi:10.20944/preprints202505.1362.v1

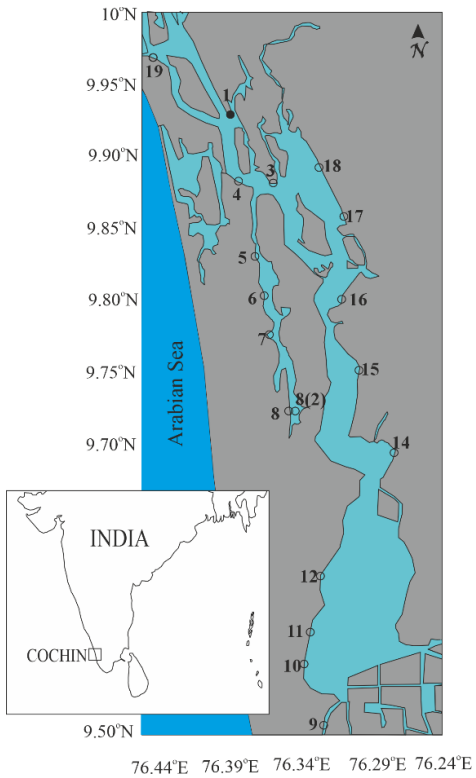

Figure 1. Map of the Cochin backwater with sampling locations. Temporal sampling location is given in filled circles (samples in Table 1); whereas, hollow circles represent locations of spatial sampling (samples in Table 2).

Table 1. Measured salinity and oxygen isotopic composition of Cochin backwater collected biweekly during both low tide and high tides at sample site 1 as indicated in Figure 1.

Date of Sample Collection	Seasons	$\delta^{18}O_{VSMOW}$ (‰)		Salinity	
		High tide	Low tide	High tide	Low tide
4-Oct	North-East Monsoon	-2.84		0.2	
18-Oct		-1.87	-1.9	8.5	5.1
2-Nov		-1.19	-3.49	12.6	11.1
16-Nov		-4.69	-4.21	1.9	1.3
2-Dec		-2.44	-3	11.5	7.1
16-Dec		-1.15	-2.22	19.4	12.3
31-Dec		-1.15	-1.54	20	16.2
15-Jan		-0.96	-1.86	19.6	17.8
30-Jan		-1.23	-0.7	21.1	18
13-Feb	Pre-Monsoon	-0.41	-0.74	21.7	17.1
28-Feb		-0.3	-1.24	20.5	18.6
15-Mar		-0.58	-0.78	18.5	18.1
15-Apr		-0.75	-1.1	20.5	16.6
14-May		-0.72	-0.47	21.6	20.3
27-May		-1.01	-1.09	7.8	4.9
14-Jun	South West Monsoon	-3.72	-3.69	0.2	0.1
27-Jun		-3.2	-3.29	0.2	0.2
11-Jul		-2.83	-2.68	1	2.6
26-Jul		-2.66	-2.58	2.5	0.5
11-Aug		-2.26	-2.2	2.8	4
26-Aug		-2.74	-2.58	0.7	0.7
8-Sep		-2.01	-2.42	10.2	2.9
25-Sep		-5.01		0.1	

 doi:10.20944/preprints202505.1362.v1

Table 2. Hydrological parameters of Cochin backwater collected during pre-monsoon season.

Sl. No	Location	Lat (°N)	Long (°E)	Salinity (PSU)	$\delta^{18}O$ (‰ VSMOW)	$\delta^{13}C_{DIC}$ (‰ VPDB)
1	Thevara ferry	9.93	76.30	0.10	0.42	-5.60
2	Panangad	9.88	76.33	18.80	0.54	-5.64
3	Arror	9.88	76.31	17.60	0.89	-10.52
4	Kudapuram (Eramallor)	9.83	76.32	15.70	NA	-9.01
5	Kodamthuruthu (Kuthiathodu)	9.80	76.33	13.10	2.49	-9.60
6	Thykkatusherry	9.77	76.33	11.70	3.31	-11.10
7A	Vyalar	9.72	76.43	10.40	1.52	-9.62
7B	Vyalar	9.72	76.43	10.40	0.43	-8.58
8	Punnamada	9.51	76.35	2.10	0.50	-14.09
9	Aaryad	9.54	76.35	0.10	1.76	-17.23
10	Pallathuserry	9.56	76.36	0.10	0.53	-21.34
11	Muhamma	9.60	76.36	3.40	1.23	-17.03
12	Thalayazham (Puthanpalam)	9.69	76.41	10.40	2.00	-11.97
13	Vaikom	9.75	76.39	11.60	3.06	-9.33
14	Kulasekaramagalam (Mekara)	9.80	76.38	11.90	0.78	-8.04
15	Punnakkaveli (South Paravoor)	9.86	76.38	12.45	2.45	-7.74
16	Chavakakadavuamera (Udayamperoor)	9.89	76.36	16.40	1.59	-7.20
17	Fort Kochi	9.97	76.24	28.00	-1.75	-2.90

2.2. Sample collection and Analysis

Water samples were collected in 50 ml HDPE bottles and stored until analysis. Measurements were conducted using the CO_2-H_2O equilibration method [27,28] on a Thermo Fisher MAT-253 isotope ratio mass spectrometer coupled with a GasBench II. Reproducibility values for $\delta^{18}O$ were 0.08‰. Water samples were analyzed immediately after collection using a conductivity probe (Orion, range 0.1 to 42, accuracy ±0.1) connected to a Thermo Scientific Orion 5-star multi-meter. The conductivity probe was standardized with Orion conductivity standards (147 µS/cm, 1413 µS/cm, and 12.9 mS/cm). For $\delta^{13}C$-DIC, water samples were collected in glass amber bottles with butyl rubber septa, treated with 1 ml of saturated $HgCl_2$ solution to inhibit biological activity, and stored. $\delta^{13}C$-DIC was measured by acidifying 2 ml of water with 0.5 ml of 100% orthophosphoric acid [29]. Standards, including NBS19 and MARJ1, were analyzed for calibration with a standard deviation of 0.09‰ for $\delta^{13}C$ [30]. Rainfall data were obtained from the nearest weather station on Willingdon Island (latitude 9° 57' 14" N, longitude 76° 16' 06" E) (http://www.tutiempo.net).

2.3. Machine Learning Methodology

Advanced machine learning techniques were employed to estimate and predict $\delta^{18}O$ and $\delta^{13}C$ isotopic compositions and salinity in the estuary as shown in the Figure 2. The models used include GBM for feature importance analysis and capturing non-linear relationships, GPR for uncertainty quantification and high prediction accuracy, ELM for efficient processing of high-dimensional data, RBNN for modeling non-linear patterns in isotopic and hydrological data, and CART for interpretable classification of estuarine zones. In addition, established conventional machine learning techniques like RF, KNN, SVM that have been sued in established isotopic predication studies were also used to model and predict changes in isotopic composition.

 doi:10.20944/preprints202505.1362.v1

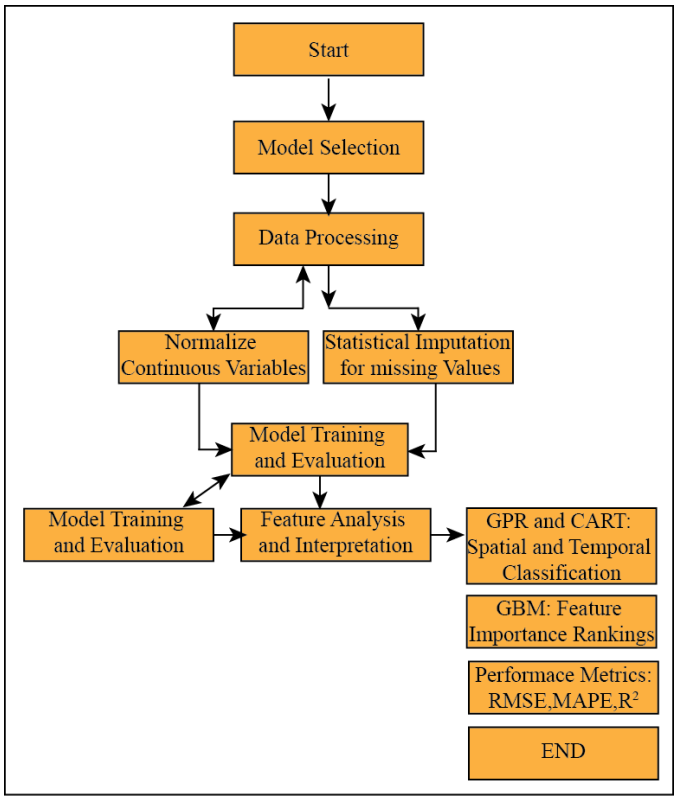

Figure 2. Work flow of advanced machine learning techniques that were employed to estimate and predict $\delta^{18}O$ and $\delta^{13}C$ isotopic compositions and salinity in the estuary.

The data preprocessing included all continuous variables, including salinity and isotopic ratios. All the data were normalized to ensure compatibility across models. All the missing values were addressed using statistical imputation methods. Model Training and Evaluation step included dividing the data into training (60%), validation (20%), and test (20%) subsets. K-fold cross-validation was employed to ensure robust model evaluation. Determination of performance metrics included Root Mean Square Error (RMSE), Mean Absolute Percentage Error (MAPE), and Coefficient of Determination (R^2). Feature Analysis and Interpretation was done using GBM, that provided feature importance rankings to identify key drivers of isotopic and salinity variations. GPR and CART enabled spatial and temporal classification of estuarine zones, revealing insights into monsoonal and non-monsoonal dynamics.

3. Results

3.1. Seasonal and Spatial Variations in $\delta^{18}O$ and Salinity

The seasonal data revealed significant oscillations in $\delta^{18}O$ and salinity values, irrespective of tidal phases as shown in Figure 3. During the North East Monsoon (NEM) period (October–December), $\delta^{18}O$ values ranged from -4.69‰ to -1.15‰, with salinity values between 20 and 0.2. The Pre-Monsoon (April–May) period exhibited $\delta^{18}O$ values from -1.1‰ to -0.47‰, with corresponding salinity values from 21.6 to 4.9. In the South West Monsoon (SWM), $\delta^{18}O$ reached its lowest value of -5‰ during low tide and increased to -1‰ during high tide. The positive correlation between $\delta^{18}O$ and salinity was evident across all seasons, though the slope of the best-fit line during the SWM was shallower than in other periods. Spatial variations were pronounced, with $\delta^{18}O$ values ranging from -1.75‰ to 3.31‰ and salinity values spanning from 0.1 to 28.0 across different stations. Salinity and isotopic values varied significantly across the studied area and three distinct zones were evident. These were classified as Zone 1 (influenced by the Periyar River): salinity ranged from 0.1 to 28.0, $\delta^{18}O$ varied between 0.7‰ and -0.6‰, and $\delta^{13}C$ ranged from -2.9‰ to -10.5‰. Zone 2 (other

 doi:10.20944/preprints202505.1362.v1

freshwater sources): salinity ranged from 10.3 to 15.7, $\delta^{18}O$ varied from 2.2‰ to -0.5‰, and $\delta^{13}C$ ranged from -7.7‰ to -11.9‰. And Zone 3 (Vembanad Lake): Salinity ranged from 0.1 to 3.4, $\delta^{18}O$ varied from 2.03‰ to -0.65‰, and $\delta^{13}C$ ranged from -14.08‰ to -21.3‰.

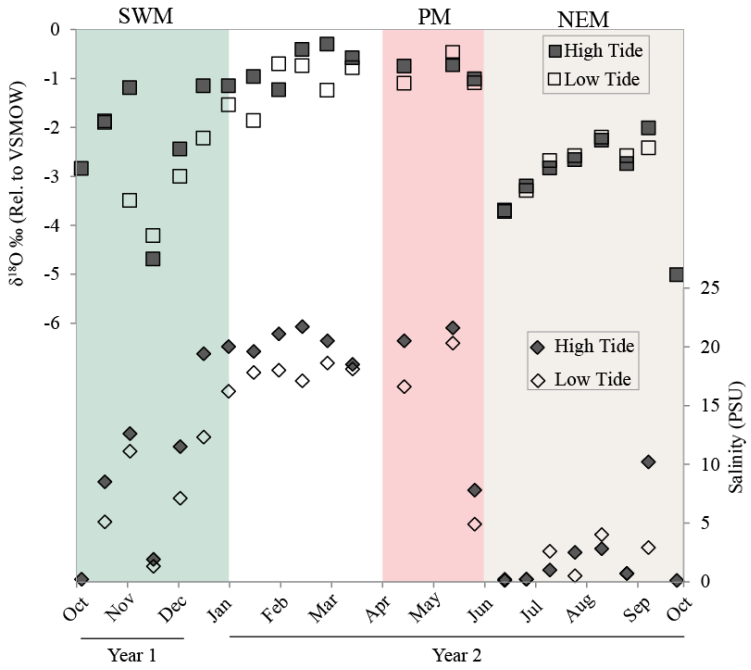

Figure 3. The top panel shows high tide and low tide water $\delta^{18}O$ measured, while the bottom panel shows salinity data measured in the collected water samples.

3.2. Performance Metrics for Machine Learning Models

The performance metrics of all the used machine learning models are summarized in Table 3. For salinity prediction, the GBM model showed the highest accuracy, with the lowest RMSE (0.0993) and the highest R^2 (0.9563). For $\delta^{18}O$ prediction, the KNN model performed best, achieving an RMSE of 0.1703, an R^2 of 0.5039, and a MAPE of 29.87%. The RF model also showed competitive performance (RMSE: 0.2101, R^2: 0.2451), while the SVM model exhibited lower predictive power with reduced R^2 values. For $\delta^{13}C$ prediction, models such as CART, ELM, and RBNN performed poorly, with negative R^2 values suggesting overfitting or insufficient training data. Low tide salinity was identified as the most significant predictor for high tide salinity in the GBM model. Geographic factors, including latitude and longitude, played a crucial role in $\delta^{18}O$ and $\delta^{13}C$ predictions. Models like GPR, CART, and RBNN also displayed negative R^2 values, indicating the necessity for further dataset expansion and model refinement.

Table 3. Performance Metrics of all machine learning models used in the study and the target parameter modelled.

Model	Target	RMSE	R^2	MAPE (%)	T-Test (p-value)
GBM	Salinity	0.0993	0.9563	N/A	<0.001
GPR	$\delta^{18}O$	0.6298	-5.7860	N/A	0.045
CART	$\delta^{13}C$	0.3449	-2.0460	N/A	0.089
ELM	$\delta^{18}O$	0.9187	-13.440	N/A	0.103
ELM	$\delta^{13}C$	0.7626	-13.890	N/A	0.097
RBNN	$\delta^{18}O$	0.2869	-0.4080	N/A	<0.001
RBNN	$\delta^{13}C$	0.2626	-0.7660	N/A	<0.001
RF	$\delta^{18}O$	0.2101	0.2451	36.19	<0.001
RF	$\delta^{13}C$	0.2489	-0.5869	34.90	0.032

 doi:10.20944/preprints202505.1362.v1

SVM	$\delta^{18}O$	0.2500	-0.0695	39.16	0.071
SVM	$\delta^{13}C$	0.2556	-0.6722	25.88	0.089
KNN	$\delta^{18}O$	0.1703	0.5039	29.87	<0.001

4. Discussion

4.1. Seasonal and Spatial Variations in $\delta^{18}O$ and Salinity

The salinity-$\delta^{18}O$ relationship is a valuable tool for understanding the temporal mixing pattern of freshwater and seawater in estuaries around the world [31–33]. The surface-water salinity-oxygen isotopes of CBW showed two distinct trends defining the summer and winter composition. This large difference between salinity and water $\delta^{18}O$ is due to the mixing of a variable amount of fresh water by the rivers draining the catchment and the saline Arabian Sea water. The rainwater $\delta^{18}O$ during the monsoon season dominates the river water value, which varies between -1.0 ‰ and -3 ‰, while groundwater remains nearly invariant seasonally with a composition of -3.7 to -5.2 ‰ [34]. The seawater input into the estuary is isotopically heavier, with values between 1 and 0 ‰ in the Arabian Sea region. The difference between the salinity values measured during high and low tides was maximum during the summer season and minimum during the monsoon season. This implies that the extent of mixing of surface water is maximum in the monsoon season and minimum in the summer. The overall relationship between water $\delta^{18}O$ and salinity is defined by $\delta^{18}O = 0.1259$ (salinity) -3.31, with a regression coefficient value of 0.7 (Figure 4).

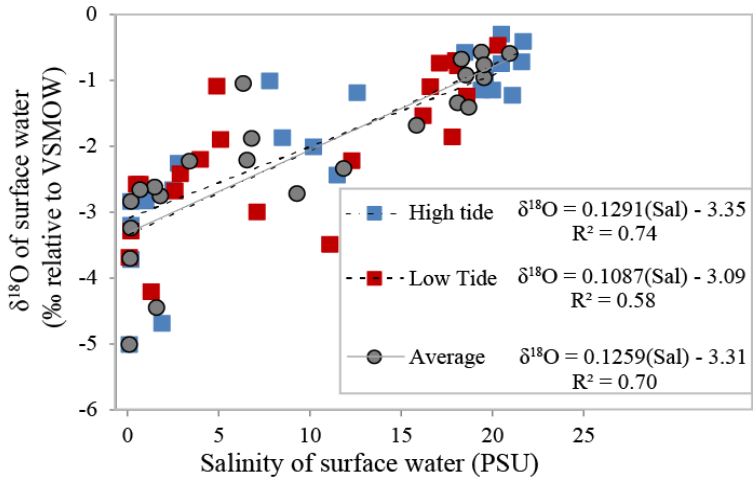

Figure 4. Correlation plot between $\delta^{18}O$ and salinity in the collected CBW samples indicating the mixing between freshwater and saline water.

4.2. $\delta^{18}O$ Relationship with Salinity

Surface water salinity depends mainly on freshwater drainage, which carries a signature of rainwater during the wet period and groundwater during the dry period. The annual salinity varies from 21.7 to 0.1 (Table 1). The lowest surface salinity coincides with a period of SWM, where precipitation and catchment runoff reach their maximum. Maximum salinity was observed during the pre-monsoon period, wherein seawater intrusion was prominent. It was evident that the CBW region experienced diurnal and monthly tidal influences, which varied seasonally with the extent of seawater intrusion into the coastal area. As a function of these influences, the CBW estuary was classified into three zones based on its physiographical and hydrographical aspects. Zone 1, the region from the Cochin inlet to Perumpalam Island, is influenced by seawater from the Arabian Sea. Zone 2, From Perumpalam Island to Thanneermukkam Bund, is characterized by the mixing of freshwater from riverine input and seawater from the Arabian Sea. Zone 3 is dominated by freshwater. As seen in Figure 5, Zone 1 has a $\delta^{18}O$-Salinity relationship slope of 0.03 with a positive

 doi:10.20944/preprints202505.1362.v1

correlation with an R^2 of 0.37. In comparison, Zone 2 had a steep slope of 0.5, with a positive correlation with an R^2 of 0.6. Zone 3 had a negative slope of -0.9 with a weak R^2 value of 0.05.

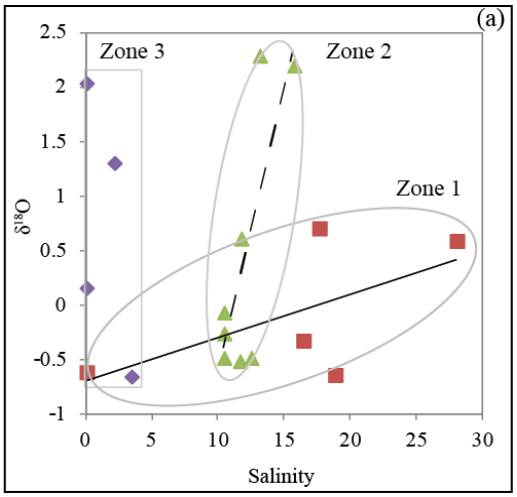

Figure 5. $\delta^{18}O$-Salinity relationship indicating three different zones for collected pre-monsoon sample is shown.

4.3. $\delta^{18}O$-δD Relationship of CBW Estuary

A total of 17 surface water samples collected during the pre-monsoon season were analyzed for δD and $\delta^{18}O$. The results are plotted in Figure 6 and compared with the Global Meteoric Water Line (GMWL) and the Local Meteoric Water Line (LMWL) from published literature [35]. In a previous study, the stable isotopes of Vembanad Lake water samples have been documented to range from -20.2 to +17.0 ‰ and -5.6 to +3.3 ‰ for δD and $\delta^{18}O$, respectively [11]. The most isotopically depleted values were observed during the monsoon season, which could be attributed to the amount effect. In contrast, an enrichment in isotopic values was observed during the pre-monsoon period due to salinity mixing or evaporation. In our study, we carried out spatial sampling only during the pre-monsoon season, and the δD vs. $\delta^{18}O$ plot is characterized by enriched δ values similar to earlier observations as shown in Figure 6 [11]. The ingression of saline seawater with enriched isotope values also contributed to overall isotope observations in the estuary. The gradual decrease in the $\delta^{18}O$ and δD values suggests that either excess evaporation or the enhanced contribution of seawater caused a compositional shift during the pre-monsoon season.

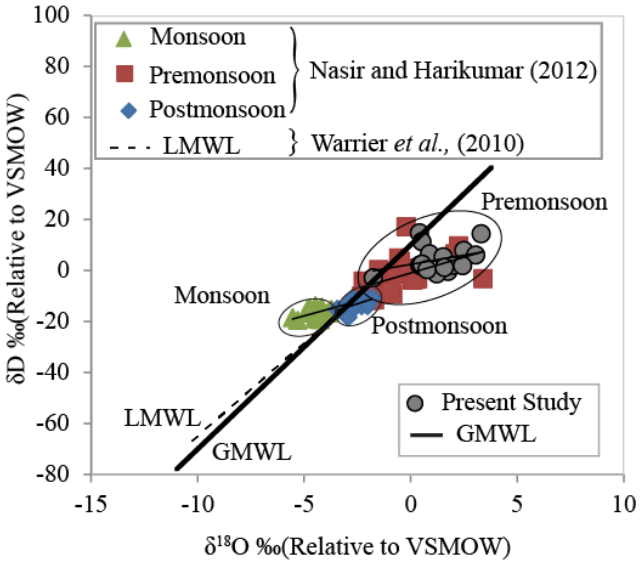

 doi:10.20944/preprints202505.1362.v1

Figure 6. Comparison of $\delta^{18}O$-δD regression line based on 18 surface water samples (Table 1) collected and compared with GMWL and LMWL.

4.4. Freshwater Flux in Comparison with the Seasonal Rainfall

In an estuarine setting, the source of freshwater can vary and each of these freshwater sources have unique $\delta^{18}O$ values, although the salinity of these sources is minimal. Previously reported $\delta^{18}O$ values of the NEM from this region are -10‰ and -2‰ for the Premonsoon and -5‰ for the SWM [25,35]. These values are close (-1.8 to -5‰) to the river water composition measured at a seasonal interval in the region [34]. Using these $\delta^{18}O$ values as freshwater end members, and measured average $\delta^{18}O$ of estuarine waters, the relative contribution of freshwater can be ascertained using the below mass balance equation.

$$F_{sw} \times \delta^{18}O_{sw} + F_{rw} \times \delta^{18}O_{rw} = \delta^{18}O_{ew} \quad (1)$$

$$F_{sw} + F_{rw} = 100 \quad (2)$$

$$\text{Percentage (\%)} = [\delta^{18}O_{ew} - \delta^{18}O_{sw}]/ [\delta^{18}O_{rw} - \delta^{18}O_{sw}] \quad (3)$$

where sw, rw, and ew refer to seawater, rainwater, and estuarine water, respectively, and F indicates the flux parameter.

The region receives rainfall distributed across three distinct rainfall seasons and is characterized by unique isotopic ratios [25,35,36]. The monthly mean and daily rainfall data of the study region was obtained from the Willingdon station, located ~3 km from the site of monthly observation. The indicated that in almost all years, rainfall is maximum from June to August coinciding with the SW monsoon (Figure 7 - Bottom panel). Based on the amount of rainfall and $\delta^{18}O$ offset, the percentage contribution of freshwater was estimated and is shown in Figure 7 (Top panel). It was evident that freshwater flux into CBW estuary is primarily driven by runoff, which is major contributor during the monsoon season but drops significantly during the pre-monsoon and post-monsoon periods The water $\delta^{18}O$ values of seasonal surface water was adapted from the tropical Chaliyar River basin to constrain the end-member composition. The catchment of this river is the Western Ghats in India, which receives the same rain source that feeds the rivers flowing into the Cochin estuary [34]. The surface water δ18O values for the river were -1.8 ‰, -1.2 ‰, and -4.5 ‰ for the NE monsoon, pre-monsoon, and monsoon seasons, respectively, while the freshwater percentages estimated were 25 %, 73 %, and 92 %, respectively. Furthermore, the estimates indicated that the fractional contribution (in %) of freshwater varies from 20-52 to% during the NE monsoon, 53-67 % during the pre-monsoon, and 50-100 % during the monsoon. High tide (HT) allows more seawater mixing in comparison to low tides.

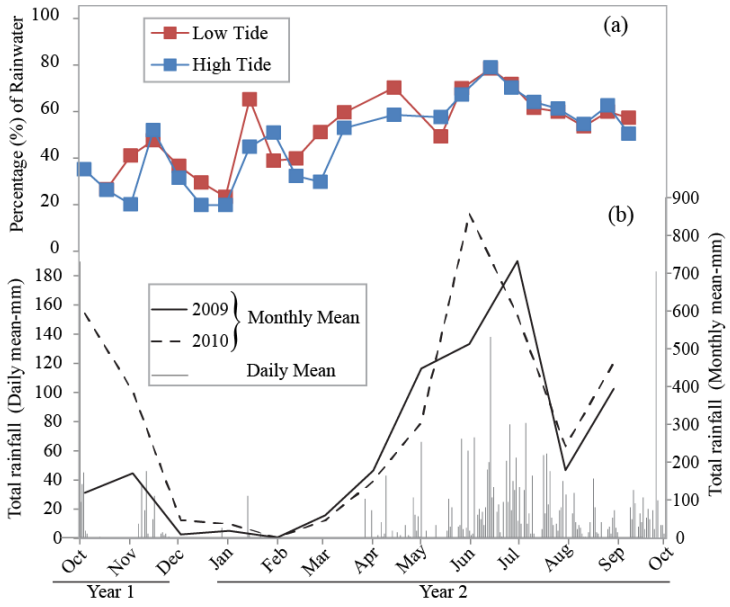

 doi:10.20944/preprints202505.1362.v1

Figure 7. Relative contribution of freshwater to the Cochin backwater at different times of the year calculated using $\delta^{18}O$ of the freshwater end-member (Seasonal rainwater $\delta^{18}O$) and seawater.

4.5. Carbon Dynamics Using Salinity and $\delta^{13}C_{DIC}$

Freshwater input to the estuary affects the net carbon isotopic composition of dissolved inorganic carbon, which is either derived from the degradation of organic matter present in the regional soil ecosystem or further modified due to water column productivity. Thus, $\delta^{13}C_{DIC}$ acts as a proxy for productivity in estuarine systems. However, the inorganic carbon reservoir in estuary water varies throughout the season, recording the flux of carbon due to silicate weathering [36]. The $\delta^{13}C_{DIC}$ observed during the present study (-2.9 ‰ to -21.34 ‰), with an average of -10.36 ‰, is comparable to a previous study in the region [12,37]. Figure 8 shows the conservative mixing curve of $\delta^{13}C_{DIC}$, along with their respective actual values and salinity in three different zones of the Cochin Estuary. Among the five stations sampled in Zone 1, four stations were generally closer to the conservative mixing line, indicating the role of mixing of freshwater and seawater end members. The samples from Zone 2 were characterized by lower $\delta^{13}C_{DIC}$ values relative to the respective conservative mixing curve values. As observed in previous studies [12,37], the possible reason for the low $\delta^{13}C_{DIC}$ at these stations might be the dominant contribution from terrestrial inorganic carbon from the degradation of organics. The samples from Zone 3 are characterized by a lower $\delta^{13}C_{DIC}$ relative to the respective conservative mixing curves. This indicates that the carbon dynamics in Zone 3 are dictated by the runoff from the nearby paddy fields with a lighter C_3 signature (-25 ‰), which is further modified owing to the productivity of the estuary [38].

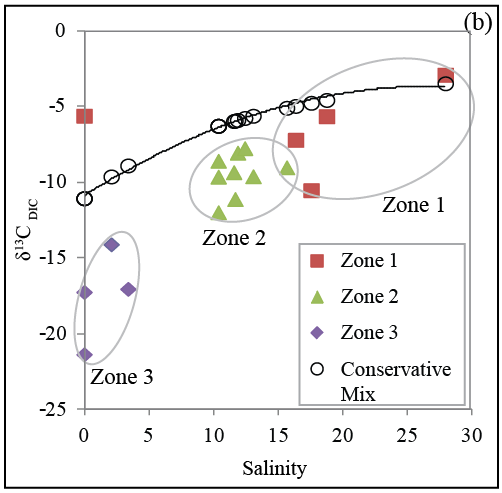

Figure 8. $\delta^{13}C$-Salinity relationship along with the conservative mixing curve for CBW estuary.

4.6. Evaluating Machine Learning Models for Salinity and Isotopic Predictions

The study compared multiple machines learning models, including GBM, KNN, RF, SVM, CART, ELM, and RBNN, to predict salinity and isotopic ratios. The study's comparison of various machine learning models highlights the challenges and opportunities in predicting salinity and isotopic compositions [15,16]. The GBM model emerged as the most reliable for salinity prediction, demonstrating the highest accuracy and predictive strength (Table 3). The strong performance of GBM can be attributed to its ability to capture complex, non-linear relationships between predictor variables, including tidal influence, temperature, and spatial factors. For $\delta^{18}O$ prediction, the KNN model outperformed others, although overall performance metrics indicated room for improvement. The low performance of models like SVM for $\delta^{18}O$ prediction suggests that certain machine learning approaches may not be well-suited for isotopic modeling without extensive parameter tuning and preprocessing (Table 3).

 doi:10.20944/preprints202505.1362.v1

$\delta^{13}C$ prediction faced significant challenges, with models like CART, ELM, and RBNN yielding negative R^2 values, suggesting overfitting or insufficient training data (Table 3). The poor performance of certain models highlights the need for expanded dataset and improved feature selection to enhance predictive accuracy. Given the complexity of $\delta^{13}C$ variations, which are influenced by multiple environmental and biological factors, the integration of additional explanatory variables, such as dissolved organic carbon sources could enhance prediction accuracy. Additionally, the strong correlation between $\delta^{18}O$ and salinity reinforces the utility of isotopes in tracing hydrochemical processes. Geographic parameters could also play a crucial role in model performance, indicating spatial influences on isotopic variations. The findings emphasize that while machine learning can be a powerful tool for hydrochemical predictions, robust data collection and model refinement are essential to improve generalizability and reliability across different environmental conditions.

5. Conclusions

The current study analyzed the seasonal variations in freshwater flux and isotopic compositions in the Cochin Backwater Estuary (CBW). It sheds light on the intricate interactions between monsoonal rains, salinity, and the use of stable isotopic markers and machine learning models. Seasonal monitoring revealed that the monsoon season contributes significantly (~77%) to the freshwater flux due to intense rainfall and riverine input, making the estuary predominantly freshwater during this period. The seasonal isotopic fingerprints revealed significant geographical and temporal patterns of intermixing at high and low tides. Detailed studies of $\delta^{13}C$ in dissolved inorganic carbon (DIC) at 17 locations throughout the pre-monsoon season indicated regional diversity and zonation in biogeochemical processes. Zone 1 is predominantly impacted by saltwater enriched in $\delta^{13}C_{DIC}$, whereas Zone 2 reflects terrestrial input from local sources. Zone 3 revealed the input of terrestrial runoff, mainly from rice fields, with lighter C_3 plant signatures, which were further influenced by estuarine productivity. Comparison of the Local Meteoric Water Line to the Global Meteoric Water Line revealed the impacts of salinity mixing and evaporation, particularly during the pre-monsoon season, providing important insights into estuarine hydrology. In addition, we used machine learning models to improve our understanding of the predictive relationships between $\delta^{18}O$, salinity, and seasonal freshwater fluxes. The used models accurately captured the nonlinear dynamics of estuarine systems, providing powerful tools for analyzing the effects of seasonal variability and salinity mixing (GBM, KNN) on estuarine ecosystems. The study's comparison of various machine learning models highlights that although machine learning could be a powerful tool for hydrochemical predictions, robust data collection and model refinement are crucial for improving reliability. In conclusion, the findings highlight the CBW's distinctive function as an ecological hotspot in southern India, where monsoon and terrestrial inputs influence biogeochemical and production dynamics. The current study not only enhances our understanding of estuarine processes in the CBW but also provides a framework for employing advanced analytical and machine learning approaches in coastal ecosystem research.

Author Contributions: Conceptualization, P.K., P.G. and R.R.; methodology, H.R., P.K., F.T.; writing—original draft preparation, P.K., R.R., P.G. and H.R.; writing—review and editing, R.R. and P.K. All authors have read and agreed to the published version of the manuscript.

Funding: This research received no external funding.

Data Availability Statement: The data presented in this study are available on request from the corresponding author.

Acknowledgments: The authors are thankful to all the help obtained during the sampling and analysis throughout the project from the project members. RR is thankful to the research support provided through the grant CCEC01-1108-230167 from Qatar Research Development and Innovation Council.

 doi:10.20944/preprints202505.1362.v1

Conflicts of Interest: The authors declare no conflicts of interest.

Abbreviations

The following abbreviations are used in this manuscript:

CBW	Cochin Back Water
DIC	Dissolved Inorganic Carbon
PM	Pre-Monsoon
SWM	South West Monsoon
NEM	Northeast Monsoon
HT	High Tide
LT	Low Tide
NBS19	National Bureau of Standards -19
HDPE	High Density Polyethylene
ANN	Artificial Neural Networks
ANFIS	Adaptive Neuro-Fuzzy Inference Systems
SVM	Support Vector Machines
RBNN	Radial Function Based Neural Network
RF	Random Forest
KNN	K-Nearest Neighbor
GBM	Gradient Boosting Machines
GPR	Gaussian Process regression
CART	Classification and Regression Tree
ELM	Extreme Learning Machines
RMSE	Root Mean Square Error
MAPE	Mean Absolute Percentage Error

References

1. Day Jr, J.W., Kemp, W.M., Yáñez-Arancibia, A. and Crump, B.C. eds., 2012. Estuarine ecology. John Wiley & Sons.
2. Dittmar, T. and Lara, R.J., 2001. Driving forces behind nutrient and organic matter dynamics in a mangrove tidal creek in North Brazil. Estuarine, Coastal and Shelf Science, 52(2), pp.249-259.
3. Cloern, J.E. and Jassby, A.D., 2010. Patterns and scales of phytoplankton variability in estuarine–coastal ecosystems. Estuaries and coasts, 33, pp.230-241.
4. Vijith V, Sundar D, Shetye SR (2009) Time-dependence of salinity in monsoonal estuaries. Estuar Coast Shelf Sci 85:601–608. doi: https://doi.org/10.1016/j.ecss.2009.10.003
5. Qasim S, Gopinathan C (1969) Tidal cycle and the environmental features of Cochin Backwater (a tropical estuary). Proc Indian Acad Sci - Sect A Part 3, Math Sci 69:336–348. doi: 10.1007/BF03051729
6. Haldar, R., Khosa, R., Gosain, A.K. (2019). Impact of Anthropogenic Interventions on the Vembanad Lake System. In: Rathinasamy, M., Chandramouli, S., Phanindra, K., Mahesh, U. (eds) Water Resources and Environmental Engineering I. Springer, Singapore. https://doi.org/10.1007/978-981-13-2044-6_2
7. Kulk, G., George, G., Abdulaziz, A., Menon, N., Theenathayalan, V., Jayaram, C., Brewin, R. J., & Sathyendranath, S. (2020). Effect of Reduced Anthropogenic Activities on Water Quality in Lake Vembanad, India. Remote Sensing, 13(9), 1631. https://doi.org/10.3390/rs13091631
8. Pranav, P., Roy, R., Jayaram, C., D'Costa, P. M., Choudhury, S. B., Menon, N. N., Nagamani, P., Sathyendranath, S., Abdulaziz, A., Sai, M. S., Sajhunneesa, T., & George, G. (2021). Seasonality in carbon chemistry of Cochin backwaters. Regional Studies in Marine Science, 46, 101893. https://doi.org/10.1016/j.rsma.2021.101893
9. Shivaprasad A, Vinita J, Revichandran C, et al. (2013) Seasonal stratification and property distributions in a tropical estuary (Cochin estuary, west coast, India)
10. Ghosh P, Chakrabarti R, Bhattacharya SK (2013) Short- and long-term temporal variations in salinity and the oxygen, carbon and hydrogen isotopic compositions of the Hooghly Estuary water, India. Chem Geol 335:118–127. doi: 10.1016/j.chemgeo.2012.10.051

 doi:10.20944/preprints202505.1362.v1

11. Nasir UP, Harikumar PS (2012) Hydrochemical and isotopic investigation of a tropical wetland system in the Indian sub-continent. Environ Earth Sci 66:111–119
12. Bhavya PS, Kumar S, Gupta GVM, et al. (2016) Carbon isotopic composition of suspended particulate matter and dissolved inorganic carbon in the Cochin estuary during post-monsoon. Curr Sci 110:
13. Raymond, P.A., Bauer, J.E., Caraco, N.F., Cole, J.J., Longworth, B. and Petsch, S.T., 2004. Controls on the variability of organic matter and dissolved inorganic carbon ages in northeast US rivers. Marine chemistry, 92(1-4), pp.353-366.
14. Bouillon, S., Borges, A.V., Castañeda-Moya, E., Diele, K., Dittmar, T., Duke, N.C., Kristensen, E., Lee, S.Y., Marchand, C., Middelburg, J.J. and Rivera-Monroy, V.H., 2008. Mangrove production and carbon sinks: a revision of global budget estimates. Global biogeochemical cycles, 22(2).
15. Astray, G., Soto, B., Barreiro, E., Gálvez, J. F., & Mejuto, J. C. (2021). Machine learning applied to the oxygen-18 isotopic composition, salinity and temperature/potential temperature in the mediterranean sea. Mathematics. https://doi.org/10.3390/math9192523.
16. Cemek, B., Arslan, H., Küçüktopcu, E., & Simsek, H. (2022). Comparative analysis of machine learning techniques for estimating groundwater deuterium and oxygen-18 isotopes. Stochastic Environmental Research and Risk Assessment. https://doi.org/10.1007/s00477-022-02262-7
17. Noori, N., Kalin, L., & Isik, S. (2020). Water quality prediction using SWAT-ANN coupled approach. Journal of Hydrology. https://doi.org/10.1016/j.jhydrol.2020.125220
18. Ly, Q. V., Nguyen, X. C., Lê, N. C., Truong, T. D., Hoang, T. H. T., Park, T. J., ... & Hur, J. (2021). Application of Machine Learning for eutrophication analysis and algal bloom prediction in an urban river: A 10-year study of the Han River, South Korea. Science of The Total Environment, 797, 149040.
19. Samalavičius, V., Gadeikienė, S., Žaržojus, G., Gadeikis, S., & Lekstutytė, I. (2024). Oxygen-18 prediction using machine learning in the Baltic Artesian Basin groundwater. Stochastic Environmental Research and Risk Assessment, 1-23.
20. Albuquerque, L. G., de Oliveira Roque, F., Valente-Neto, F., Koroiva, R., Buss, D. F., Baptista, D. F., Hepp, L. U., Kuhlmann, M. L., Sundar, S., Covich, A. P., & Pinto, J. O. P. (2021). Large-scale prediction of tropical stream water quality using Rough Sets Theory. Ecological Informatics. https://doi.org/10.1016/j.ecoinf.2021.101226
21. Al Sudani, Z. A., & Salem, G. S. A. (2022). Evaporation rate prediction using advanced machine learning models: a comparative study. Advances in Meteorology, 2022(1), 1433835.
22. Dagher, D. H. (2024). Assessment of Using Machine and Deep Learning Applications in Surface Water Quantity and Quality Predictions: A Review. Journal of Water Resources and Geosciences, 3(2), 18-48.
23. Singh A, Jani RA, Ramesh R (2010) Spatiotemporal variations of the δ18O-salinity relation in the northern Indian Ocean. Deep Sea Res Part I Oceanogr Res Pap 57:1422–1431
24. Deshpande RD, Muraleedharan PM, Singh RL, et al. (2013) Spatio-temporal distributions of δ18O, δD and salinity in the Arabian Sea: Identifying processes and controls. Mar Chem 157:144–161
25. Lekshmy, P.R., Midhun, M., Ramesh, R. and Jani, R.A., 2014. 18O depletion in monsoon rain relates to large scale organized convection rather than the amount of rainfall. Scientific reports, 4, p.5661.
26. Rasheed K, Joseph KA, Balchand AN (1995) Impacts of harbour dredging on the coastal shoreline features around Cochin. In: Proceedings of the international conference on 'Coastal Change. pp 943–948
27. Epstein S, Mayeda T (1953) Variation of O18 content of waters from natural sources. Geochim Cosmochim Acta 4:213–224
28. Rangarajan R, Ghosh P (2011) Role of water contamination within the GC column of a GasBench II peripheral on the re-producibility of 18O/16O ratios in water samples. Isotopes Environ Health Stud 47:498–511
29. Assayag N, Rivé K, Ader M, et al. (2006) Improved method for isotopic and quantitative analysis of dissolved inorganic carbon in natural water samples. Rapid Commun Mass Spectrom 20:2243–2251. doi: https://doi.org/10.1002/rcm.2585
30. Rangarajan, R., Pathak, P., Banerjee, S. and Ghosh, P. (2021). Floating boat method for carbonate stable isotopic ratio determination in a GasBench II peripheral. Rapid Communications in Mass Spectrometry, 35(15), p.e9115.

 doi:10.20944/preprints202505.1362.v1

31. Torgersen T (1979) Isotopic composition of river runoff on the US East Coast: Evaluation of stable isotope versus salinity plots for coastal water mass identification. J Geophys Res Ocean 84:3773–3775
32. Fairbanks RG, Sverdlove M, Free R, et al. (1982) Vertical distribution and isotopic fractionation of living planktonic forami-nifera from the Panama Basin. Nature 298:841
33. Khim B-K, Park B-K, Yoon H Il (1997) Oxygen isotopic compositions of seawater in the Maxwell Bay of King George Island, west Antarctica. Geosci J 1:115
34. Hameed AS, Resmi TR, Suraj S, et al. (2015) Isotopic characterization and mass balance reveals groundwater recharge pattern in Chaliyar river basin, Kerala, India. J Hydrol Reg Stud 4:48–58. doi: https://doi.org/10.1016/j.ejrh.2015.01.003
35. Rahul, P. and Ghosh, P., 2019. Long term observations on stable isotope ratios in rainwater samples from twin stations over Southern India; identifying the role of amount effect, moisture source and rainout during the dual monsoons. Climate Dynamics, 52(11).
36. Warrier, C.U., Babu, M.P., Manjula, P., Velayudhan, K.T., Hameed, A.S. and Vasu, K., 2010. Isotopic characterization of dual monsoon precipitation–evidence from Kerala, India. Current Science, pp.1487-1495.
37. Samanta S, Dalai TK, Tiwari SK, Rai SK (2018) Quantification of source contributions to the water budgets of the Ganga (Hooghly) River estuary, India. Mar Chem 207:42–54. doi: 10.1016/j.marchem.2018.10.005
38. Bhavya PS, Kumar S, Gupta GVM, et al. (2018) Spatio-temporal variation in δ13CDIC of a tropical eutrophic estuary (Cochin estuary, India) and adjacent Arabian Sea. Cont Shelf Res 153:75–85. doi: https://doi.org/10.1016/j.csr.2017.12.006
39. Kaushal R, Ghosh P, Geilmann H (2016) Fingerprinting environmental conditions and related stress using stable isotopic composition of rice (Oryza sativa L.) grain organic matter. Ecol Indic 61:941–951. doi: https://doi.org/10.1016/j.ecolind.2015.10.050